Experimental Analysis of Flow Through Throttle Valve During Gaseous Cavitation

Tomáš Polášek[1,*], *Lumír* Hružík[1], *Adam* Bureček[1] and *Marian* Ledvoň[1]

[1]VSB-Technical University of Ostrava, Faculty of Mechanical Engineering, Department of Hydromechanics and Hydraulic Equipment, 17. listopadu 2172/15, 708 00 Ostrava-Poruba, Czech Republic

Abstract. The multiphase flow in oil hydraulic systems has a very significant effect on the correct operation of the hydraulic system. Air can be found in various states in hydraulic systems, while free entrained air in the form of bubbles has the potential to be the most problematic. It especially affects the compressibility of the hydraulic liquid resulting in reduced stiffness of the hydraulic system. The actuators of the hydraulic mechanisms then do not achieve the fast response and the precision of movements depending on the input control signals. One possibility for the contamination of hydraulic fluid by air bubbles is through a phenomenon known as gaseous cavitation. This is a phenomenon in which gas is released when the pressure drops below the saturation pressure of the dissolved gas in the liquid. This article focuses on the experimental analysis of the flow through the throttle valve which is affected by the formation of air bubbles at the throttle edge of the valve. The regions of gaseous cavitation were observed at the different flow cross-section of the throttle valve. The throttle valve was placed into the block of transparent material to provide visualization of the individual measurements. The article is supplemented with photographs of the individual measurements showing the gaseous cavitation inception.

Research background: flow cross-section, cavitation phenomenon, discharge coefficient.
Purpose of the article: Effect of flow cross-section size and flow velocity on cavitation development.
Methods: Experimental measurements.
Findings & Value added: The investigation of the gaseous cavitation inception, Visualization of the individual measurements.

Keywords: *throttle valve, cavitation number, discharge coefficient, saturation pressure*, *visualization*

* Corresponding author: tomas.polasek@vsb.cz

1 Introduction

The throttle valves are variable hydraulic resistances that can be used to control the amount of flow rate. When the liquid passes through these throttle elements, there is significant pressure loss depending on the size of the flow cross-section. These pressure losses have a significant effect on the energy balance of hydraulic systems [1]. Due to the significant change in the flow cross-section, a large increase of the flow velocity occurs on the flow control elements which causes a local decrease of the static pressure. At these location, the gaseous and vapour cavitation can be expected.

All hydraulic liquids, including oil, contain a specific amount of air. The air can be considered as a contaminant in hydraulic equipment which changes the properties of the working fluid and the hydraulic mechanism [2-4]. Therefore, air can exist in different states. While the most discussed is the free entrained air in the form of small bubbles. One of the possibilities of hydraulic equipment contamination by free entrained air is leakage of individual connections in the suction line of the pumps. Due to the insufficient tightness of the sealing surfaces, the air is drawn in by the vacuum in the suction line and entrained into the working areas of the pumps. Another possibility of the hydraulic equipment contamination is due to a phenomenon known as gaseous cavitation. The cause of gas cavitation in hydraulic systems is very similar to the vapour cavitation. The difference between these two phenomena is in the contained gases in the formed cavities. The vapour cavitation occurs when the pressure drops below the saturation vapour pressure of the liquid. The process of evaporation and formation of vapour bubbles occurs including a small amount of non-condensable gas (air) at the given temperature [5]. It is similar in the gaseous cavitation. When the pressure drops below the level of the saturation pressure of the dissolved gas in the liquid, the gas is released at the given temperature. These are different physical processes that occur in liquids. While the vapour cavitation is accompanied by the phase change between liquid and gas phases, gas cavitation is associated with diffusion processes in the liquid [2, 11]. Liquids are affected by both processes [6-9], and both significantly affect the hydraulic mechanisms.

The hydraulic oils also exhibit both gaseous and vapour cavitation [8-11], but the conditions for the release of oil vapour bubbles are more difficult to achieve in comparison to the release of water vapour bubbles. This is due to the different properties of the liquids, which are manifested, among other things, by the very low saturation vapour pressure of the oil. This can vary depending on the operating temperature range, additives added, type of hydraulic oil, etc. However, gaseous cavitation, which is influenced by the amount of dissolved gas in the liquid, is far more common in the oil hydraulic systems. The hydraulic oils can contain much more dissolved air (up to 10 %) in comparison to the water [2]. The amount of dissolved gas in the liquid is directly proportional to the partial pressure of the gas in the liquid which is related by Henry's law. Thus, the solubility of gas in liquids depends on temperature and pressure. Due to the constant changes in pressure and temperature in hydraulic systems, gas is absorbed or released to maintain this equilibrium state.

2 Theoretical background

Contamination of the hydraulic fluid with air occurs already in the tank where the gas dissolves at atmospheric pressure at the interface between the hydraulic liquid and air. The amount of dissolved gas depends on temperature, pressure and it is described by Henry's law. This law states that when a gaseous mixture is in contact with a liquid, the amount of any dissolved gas in the gaseous mixture is directly proportional to the partial pressure of the given gas above the surface. The mathematical description of this law has many forms, and therefore the resulting values and dimensions of Henry's constant vary depending on the

formula used. The individual formulas are summarized in the literature [12]. The example of mathematical description of the Henry's law is as follows [12]:

$$x_{G,i} = H^{xp} \cdot p_{G,i}\,, \tag{1}$$

where $x_{G,I}$ is the molar fraction of the i-th dissolved gas in the liquid, H^{xp} is the Henry's constant which depends on the temperature and the given gas/liquid combination, $p_{G,i}$ is the partial pressure of the i-th gas above the surface. The partial pressure of the given gas is a fraction of the total mixture pressure with respect to the given gas content in the mixture. This is described by Dalton's law:

$$p_{G,i} = p_{total} \cdot x_{G,i}\,, \tag{2}$$

where p_{total} is the total pressure of the mixture. The gases with a very small fraction in the mixture are neglected in the calculations.

When the hydraulic oil passes through the throttle edges of the valve or orifice, the flow velocity increases and the static pressure drops. This correlation between flow velocity and static pressure can be described by Bernoulli's equation which states that the total energy at any point of the flow is constant. At the location of the narrowest flow area, there is the greatest flow velocity increase and the greatest static pressure decrease at the same time. Therefore, the vapour and gaseous cavitation formation is assumed to occur at this location. The cavitation number has been introduced to quantitatively evaluate the cavitation [13, 14]. The cavitation number is based on the knowledge of the pressure coefficient C_p, where at some point of the flow field, the static pressure is reduced so that the condition is reached [13]:

$$p_{\min} \le p_v\,, \tag{3}$$

where p_{min} is the minimum static pressure in the flow field, p_v is the saturation vapour pressure of the liquid. In order to evaluate gaseous cavitation formation when the liquid passes through the throttle valve, the relations were considered where instead of the saturation vapour pressure p_v, the saturation pressure p_{sat} of the dissolved gases was considered. Thus, the dimensionless cavitation number has the resulting relation [13, 14]:

$$\sigma = \frac{2 \cdot \left(p_1 - p_{sat}\right)}{\rho \cdot v_{CS}^{\,2}}\,, \tag{4}$$

where p_1 is the measured absolute upstream pressure of the throttle valve, p_{sat} is the saturation pressure of the dissolved gases, ρ is the oil density at the given temperature and v_{CS} is the flow velocity at the narrowest flow cross-section. In general, this parameter can be characterized as the ratio of the force trying to suppress cavitation to the force trying to cause it [14]. In the case of flow through the valve, the flow velocity in the dynamic pressure expression can be related directly to the pressure drop Δp [15]. Pressure drop can be measured directly on the valve being investigated. Thus, the cavitation number can be modified into the following form of the cavitation index [10, 14, 15]:

$$\sigma_v = \frac{p_1 - p_{sat}}{\Delta p}\,, \tag{5}$$

where Δp is the pressure drop of the valve. The assumption was considered in the definition of p_{sat}. When the pressure drops about 40 000 Pa, relative to the atmospheric pressure, there is a violent release of air bubbles [17]. Therefore, the value of the saturation pressure of the dissolved gases was determined to be p_{sat} = 60 000 Pa. Because of the cavitation occurrence, it is necessary to investigate the flow conditions at different valve openings and to determine the impact on the valve function or the device. The 3D model of the investigated throttle valve is shown in Fig. 1.

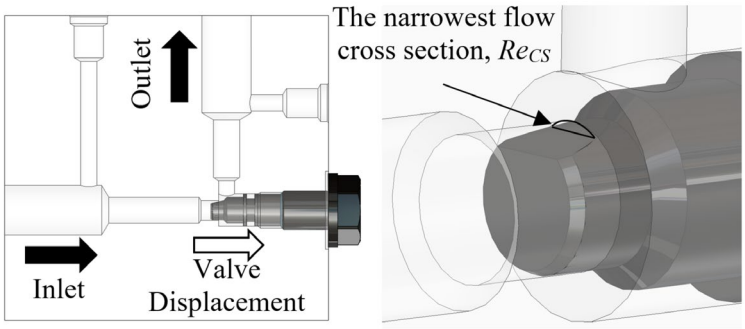

Fig. 1. The 3D model of the investigated valve.

The Reynolds number was determined to evaluate the flow regime through the valve. The Reynolds number was determined for a non-circular flow cross-section in the narrowest flow cross-section of the valve:

$$Re_{CS} = \frac{v_{CS} \cdot d_h}{\upsilon}, \tag{6}$$

where v_{CS} is the mean flow velocity in the narrowest flow cross-section, d_h is the hydraulic diameter and υ is the oil kinematic viscosity at t_O = 40 °C. In the case of a non-circular flow cross-section, the hydraulic diameter d_h was determined according to equation:

$$d_h = 4 \cdot \frac{S_{CS}}{o_{CS}}, \tag{7}$$

where S_{CS} is the non-circular flow cross-section, o_{CS} is the wetted perimeter of the flow cross-section. To characterize the loss through the valve, the loss coefficient was determined to the location of the narrowest flow cross-section [16]:

$$\zeta = \frac{2 \cdot \Delta p \cdot S_{CS}^{\ 2}}{\rho \cdot Q_v^{\ 2}}, \tag{8}$$

where Δp is the pressure drop of the valve, Q_v is the volume flow rate through the throttle valve, ρ is the oil density at the temperature of t_O = 40 °C. The flow through the throttle elements can be characterised by the equation:

$$Q_v = \mu \cdot S_{CS} \cdot \sqrt{\frac{2 \cdot \Delta p}{\rho}}, \tag{9}$$

where μ is the discharge coefficient. The discharge coefficient is in correlation with the loss coefficient and can be expressed by the following equation [16]:

$$\mu = \frac{1}{\sqrt{\zeta}} \tag{10}$$

3 Experimental measurement

The device for experimental analysis of flow through the throttle valve affected by gaseous cavitation was built. Hydraulic oil HV46 was used in the realization of the experimental measurements. For this mineral oil, the dependencies of the oil dynamic viscosity η_O and oil density ρ_O on the temperature t_O were determined. The measurement was performed in the range of oil temperature t_O = (39.5 ÷ 43.5) °C. The throttle valve was placed into the block of transparent material. Photographic images were recorded during the individual measurements using a camera with a macro lens. The images were used to evaluate

the inception of gaseous cavitation and also to evaluate the displacement of the throttle valve relative to the seat. The measurements were performed for 3 variants of the throttle valve opening VSV2-QC2/1 from Argo Hytos company. The experimental measurement was terminated when the upstream pressure p_1 = 40 bar was reached due to the strength of the transparent block. The downstream pressure p_2 was influenced by the pressure loss in the return line. Fig. 2 shows the hydraulic circuit diagram of the experimental device for flow analysis through the throttle valve including the used sensors.

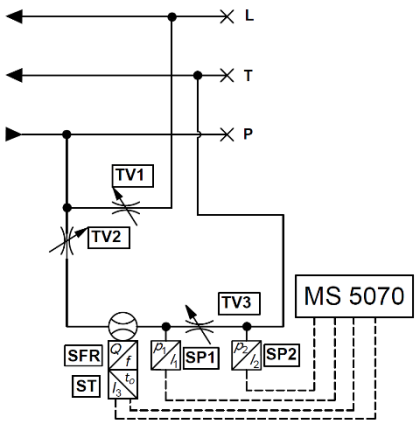

SFR	Hydrotechnik QG100. Measuring range (0.2 ÷ 30) $dm^3 \cdot min^{-1}$. Accuracy ±0.5 % of measured value.
ST	Hydrotechnik TE300. Measuring range (-50 ÷ 200) °C. Accuracy max. 0.3+0.005·t °C
SP1	Hydrotechnik PR400. Measuring range (0 ÷ 60) bar. Accuracy ±0.25 % of full scale.
SP2	Hydrotechnik PR300. Measuring range (-1 ÷ 6) bar. Accuracy 0.5 % of full scale.

Fig. 2. The hydraulic circuit diagram with the used sensors.

The hydraulic unit with an axial piston pump was the source of the flow which distributed the fluid through the high-pressure pipeline P. The amount of the volume flow rate Q_v was controlled by changing the pump speed or by changing the angle of the swash plate. Two throttle valves TV1 and TV2 were placed in the hydraulic circuit to provide flow branching. This layout was chosen to measure the characteristics in the range of the small volume flow rates, but also to achieve greater variability in adjusting the required volume flow rate Q_v. The amount of volume flow rate Q_v was measured using the gear flowmeter SFR. The temperature sensor ST was also placed on the flowmeter to record the oil temperature t_O. To evaluate the pressure drop Δp at the throttle valve TV3, pressures p_1 and p_2 were recorded using pressure sensors SP1 and SP2. The pipelines L and T were used to return the hydraulic oil into the hydraulic unit tank.

4 Experimental results

The evaluation of the displacement was performed for 3 variants of valve opening. In the camera software, the images from the measurements were analysed and the valve displacements were determined to be s = 1.31; 2.31 and 3.31 mm. Based on the displacements, the flow cross-section of the throttle valve were determined, see Fig. 3.

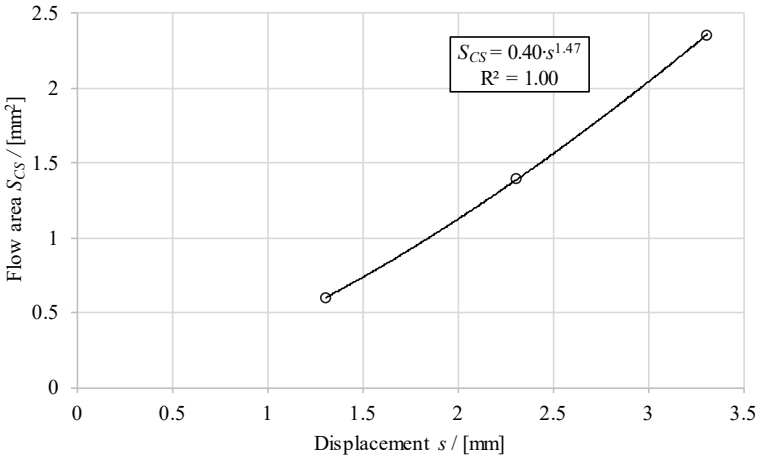

Fig. 3. The dependence of the flow cross-section S_{CS} on the throttle valve displacement s.

Because of the relatively small volume flow rates and the very low saturation vapour pressure of the oil, it can be assumed that the inception of cavitation was mainly influenced by the released air bubbles. The figure below shows the evaluation of the static Δp-Q characteristic of the flow through the throttle valve. In Fig. 4, the equations of the trend curves are evaluated and the location of the gaseous cavitation inception are marked in the form of cavitation index $\sigma_{v,i}$ for each valve displacement s ($\sigma_{v1,i}$, $\sigma_{v2,i}$, $\sigma_{v3,i}$).

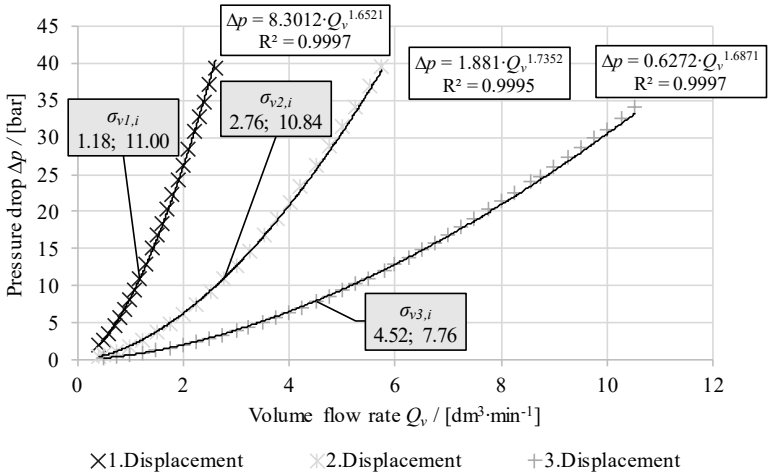

Fig. 4. The static Δp-Q characteristic of the flow through the throttle valve for different flow cross-sections S_{CS}.

In Fig. 4, it is not observed that gaseous or vapour cavitation significantly affects the static Δp-Q characteristic of the throttle valve. However, it can be observed that in the case of the 1st and the 2nd displacement, the gaseous cavitation inception occurred at approximately the same pressure drop. While for the 3rd displacement at the lower pressure drop. The images of the cavitation inception A1 to A3 and the images of the last measurement point B1 to B3 are shown in Fig. 5, also see Fig. 4.

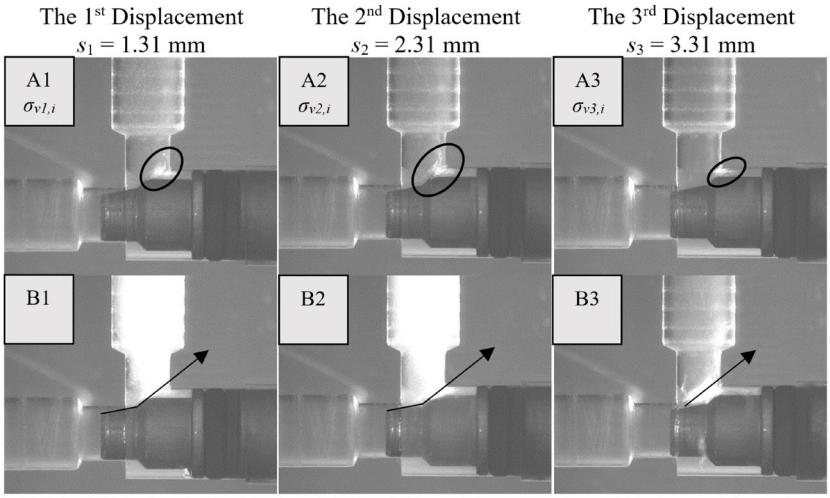

Fig. 5. The graphical evaluation of the gaseous cavitation inception at throttle valve A1, A2, A3 and cavitation at the highest achieved volume flow rates B1, B2, B3 for the individual displacements *s*.

It can be observed in Fig. 5 that for the 1st and the 2nd displacement, there was a significant increase of the gas phase downstream of the valve during the experimental measurements (see Fig. 5 - B1 and B2). While for the 3rd displacement the increase was significantly smaller (see Fig. 5 - B3). At the same time, it can be observed that a significant increase of the gas bubbles occurs in the entrainment where the flow was detached from the valve body (see Fig. 5 - A1, A2, A3). The volume fraction of the gas phase could be affected by the higher downstream pressure p_2, see Fig. 6, which increased with increasing volume flow rate Q_v, but also due to the change in the direction of the flow immediately downstream of the throttle edge of the valve. In the case of the 1st displacement, the effect of the change in flow direction was the most significant and decreased with the further displacements (see Fig. 5 - B1, B2, B3).

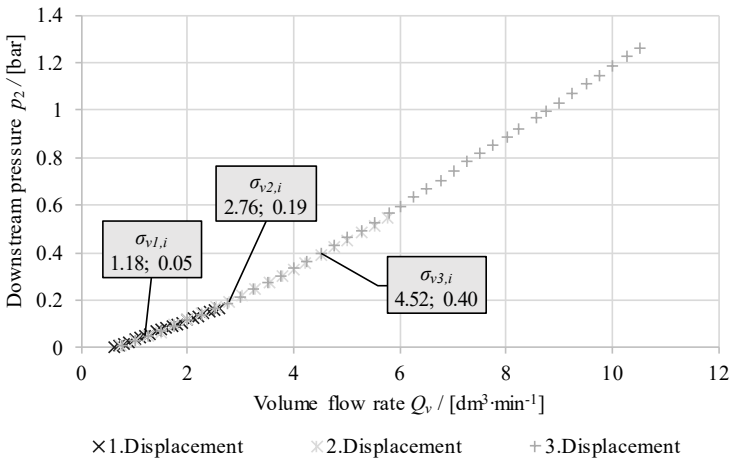

Fig. 6. The dependence of the downstream pressure p_2 on the volume flow rate Q_v.

Next, the mean flow velocities were v_{CS} evaluated and determined to the narrowest flow cross-section of the valve S_{CS}. In Fig. 7, the course of the evaluated dependencies can be observed, where the locations of the gaseous cavitation inception are marked again.

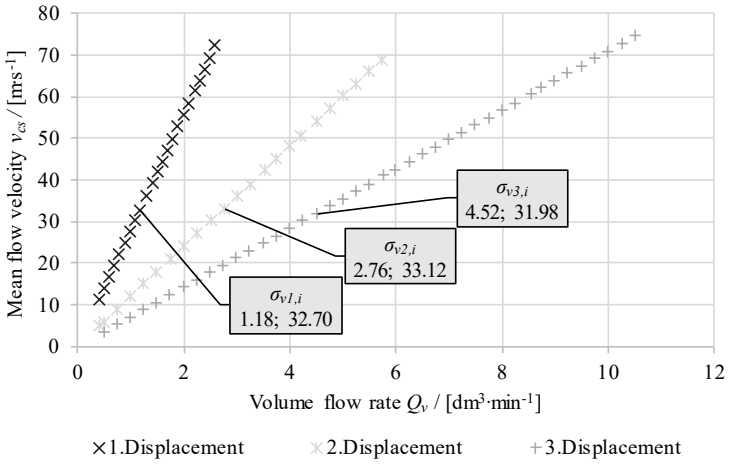

Fig. 7. The dependence of the mean flow velocity v_{CS} on the volume flow rate Q_v.

Fig. 7 shows that the gaseous cavitation inception occurred at approximately the same mean flow velocity v_{CS}. Thus, it can be assumed that the dynamic pressure in the throttle region reaches similar values as the flow cross-section S_{CS} of the throttle valve increases. As the flow cross-section S_{CS} increases, the flow velocity is dispersed more into the space. For this reason, the largest amount of gas phase can be observed at the 1st and the 2nd displacement. After the liquid passed through the throttle edge, a jet was produced which bypassed the valve until the point of break-off. In contrast, the smallest amount of gas phase can be observed at the 3rd displacement when the flow cross-section S_{CS} of the valve is the largest. For these reasons, the different intensities of air bubble release are achieved at the gaseous cavitation inception. The dependence of the discharge coefficient μ on the Reynolds number Re_{CS} was further evaluated to investigate the flow, (see Fig. 8).

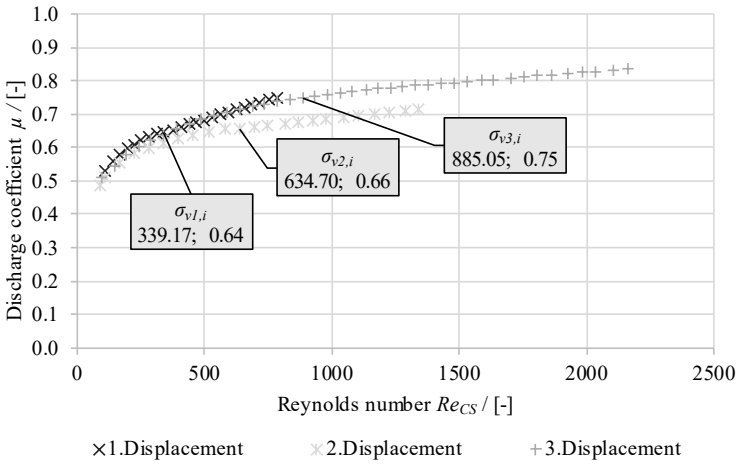

Fig. 8. The dependence of the discharge coefficient μ on the Reynolds number Re_{CS}.

It can be observed in Fig. 8 that at the gaseous cavitation inception, the value of the discharge coefficients in the case of the 1st and the 2nd displacement reached approximately the same value $\mu = (0.64 \div 0.66)$. While in the case of the 3rd displacement, it reached a higher value $\mu = 0.75$. It can be seen from the graphical dependence that in the case of the

1st and the 2nd displacement, the fluid flow was more restricted in comparison to the 3rd displacement (see Fig. 5). This condition may have occurred due to the intensity of the change in flow direction for the individual valve displacement *s*.

Finally, the cavitation indexes are evaluated. The dependence of the cavitation index σ_v on the pressure drop Δp is shown in Fig. 9. It can be observed that the gaseous cavitation inception occurred at values of the cavitation indexes $\sigma_{v,i}$ = (1.04 ÷ 1.10) depending on the valve displacement *s*.

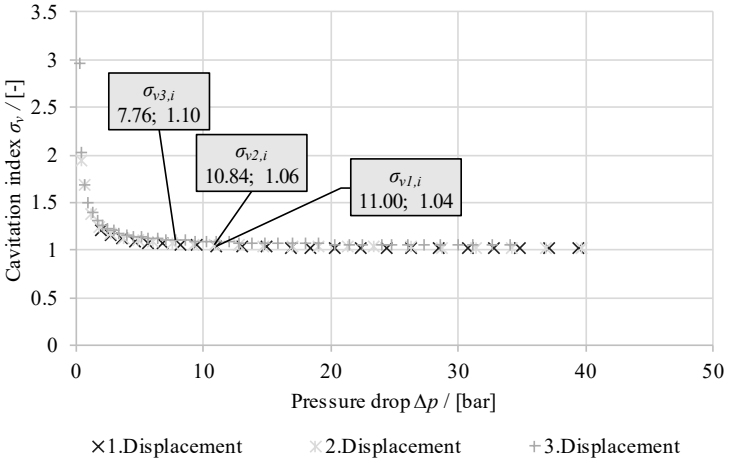

Fig. 9. The dependence of the cavitation index σ_v on the pressure drop Δp.

5 Conclusion

The article focuses on the experimental analysis of the flow through the throttle valve which was affected by cavitation. Due to the small volume flow rates and very low saturation vapour pressure of the oil, it was assumed that the cavitation inception at the valve is mainly influenced by the release of air bubbles. The gaseous cavitation inception was evaluated visually by means of a camera with a macro lens. From the evaluated static Δp-Q characteristic, it can be concluded that the release and formation of the gas cloud did not affect the change in the trend of the resulting characteristic. The inception and intensity of gaseous cavitation depends on the geometrical parameters of the valve. Depending on the position of the throttle valve, the flow was restricted not only in the narrowest cross-section of the valve, but also in the valve entrainment where the fluid flow was detached from the valve body. The largest increase of the gas phase was also observed at these locations where the relatively high flow velocity and the valve geometry resulted in swirling. This location was therefore accompanied by a local decrease of static pressure providing conditions for the air bubble expansion and further bubble release. However, the present experimental analysis does not give an idea of the amount of gas phase that was released. For future analysis, measurements with the Acoustic bubble spectrometer are planned to determine the size and number of bubbles or the volume fraction of gas in the liquid. A pressure control valve is also planned to be placed downstream of the throttle valve to achieve identical conditions at the outlet. The results of the experimental analyses can then be used as input parameters for CFD simulations in order to solve the multiphase flow of hydraulic fluid and air.

This work was supported by the European Regional Development Fund in the Research Centre of Advanced Mechatronic Systems project, project number CZ.02.1.01/0.0/0.0/16_019/0000867 within the Operational Programme Research, Development and Education.

The work presented in this paper was supported by a grant SGS „Numerical modeling of transient fluid flow problems with the support of experimental research" SP2022/32.

References

1. Vasina, M., Hruzik, L., Burecek, A. (2018). Energy and dynamic properties of hydraulic systems. *Tehnicki vjesnik-technical gazette*, 25(2), 382-390.
2. Osterland, S., Muller, L., Weber, J. (2021). Influence of Air Dissolved in Hydraulic Oil on Cavitation Erosion. *International journal of fluid power*, 22(3), 373-392.
3. Holl, E. (2022). Improvement of the modeling of a hydraulic drive for exoskeleton application based on measurements. *Materials Today: Proceedings*, 62(5), 2409-2415.
4. Burecek, A., Hruzik, L., Vasina, M. (2015). Determination of Undissolved Air Content in Oil by Means of a Compression Method. *Strojniski vestnik-journal of mechanical engineering*, 61(7-8), 477-485.
5. Himr, D., Haban, V., Zavorka, D. (2019). Axial check valve behaviour during flow reversal. In *IOP Conference Series: Earth and Environmental Science* (Vol. 405, No. 1, p. 012012). IOP Publishing.
6. Jablonska, J., Kozubkova, M., Mahdal, M., Marcalik, P., Tuma, J., Bojko, M., Hruzik, L. (2021). Spectral analysis of gaseous cavitation in water through multiphase mathematical and acoustic methods. *Physics of fluids*, 33(8), 085128.
7. Suo, XY., Jiang, Y., Wang, WJ. (2021). Hydraulic axial plunger pump: gaseous and vaporous cavitation characteristics and optimization method. *Engineering applications of comupational fluid mechanics*, 15(1), 712-726.
8. Jablonska, J., Kozubkova, M., Bojko, M. (2021). Flow of oil and water through the nozzle and cavitation. *Processes*, 9(11), 1936.
9. Yuan, C., Zhu, LS., Liu, SQ., Li, H. (2021). Examination of viscosity effect on cavitating flow inside poppet valves based on a numerical study. *Applied sciences-basel*, 11(23), 11205.
10. Iben, U., Wolf, F., Freudigmann, HA., Frohlich, J., Heller, W. (2015). Optical measurements of gas bubbles in oil behind a cavitating micro-orifice flow. *Experiments in fluids*, 56(6), 114.
11. Iben, U., Makhnov, A., Schmidt, A. (2018). Numerical study of the effects of dissolved gas release in cavitating flow. In *AIP Conference Proceedings* (Vol. 2027, No. 1, p. 030128). AIP Publishing LLC.
12. Sander, R., Acree, WE., De Visscher, A., Schwartz, SE., Wallington, TJ. (2022). Henry's law constants (IUPAC Recommendations 2021). *Pure and applied chemistry*, 94(1), 71-85.
13. Brennen, C. E. (2014). *Cavitation and bubble dynamics*. Cambridge university press.
14. Tullis, J. P. (1993). *Cavitation guide for control valves* (No. NUREG/CR-6031). Nuclear Regulatory Commission, Washington, DC (United States). Div. of Engineering; Tullis Engineering Consultants, Logan, UT (United States).
15. Martin, CS., Medlarz, H., Wiggert, DC., Brennen, C. (1981). Cavitation inception in spool valves. *Journal of fluids engineering-transactions of the ASME*, 103(4), 564-576.
16. Kudzma, Z., Stosiak, M. (2015). Studies of flow and cavitation in hydraulic lift valve. *Archives of civil and mechanical engineering*, 15(4), 951-961.
17. Sikora, R., Burecek, A., Hruzik, L., Vasina, M. (2015). Experimental investigation of cavitation in pump inlet. In *EPJ Web of Conferences* (Vol. 92, p. 02081). EDP Sciences.